Acute Neck Infections

Blair A. Winegar[1], Wayne S. Kubal[2]

We present an overview of the imaging of acute neck infections with a focus on contrast-enhanced CT. The emphasis of this chapter is to enable the emergency radiologist to accurately diagnose neck infections, to effectively communicate imaging findings with emergency physicians, and to function as part of a team offering the best care to patients.

Patients with many types of head and neck infections may present in the emergency department. The causes of these disorders include dental infection, penetrating trauma, and upper respiratory infections. Neck infections continue to portend significant morbidity and mortality despite widespread access to antibiotics. Potentially life-threatening complications may occur in approximately 10–20% of acute neck infections, including airway obstruction, septic thrombophlebitis with septic emboli, arterial pseudoaneurysm, and mediastinitis [1]. As more and more patients use emergency departments for initial healthcare, emergency department physicians will increasingly encounter acute neoplastic and nonneoplastic conditions in the head and neck [2]. In this setting, CT is the preferred imaging modality [2].

Although acute neck infections are easily diagnosed by clinical examination, correct localization may be problematic without cross-sectional imaging. The extent of deep space involvement is particularly difficult to detect by clinical evaluation, with accurate localization of infection in only 42.9% of cases in one series [3]. In another series, the extent of deep neck space infection was underestimated in 70% of cases [4]. The anatomy of the cervical fascia affects the presentation, spread, and management of neck infection [5]. Therefore, radiologists must be familiar with the anatomy of the deep cervical fascia and the spaces bounded by these fascial planes. Because the layers of the deep cervical fascia are not well seen on contrast-enhanced CT, knowledge of their normal internal contents and expected boundaries is critical [6].

The Pharyngeal Mucosal Space

The pharyngeal mucosal space is bounded by the middle layer of the deep cervical fascia and contains the mucosa of the upper aerodigestive tract and lymphoid tissue of the Waldeyer ring, including the palatine tonsils, lingual tonsils, and adenoids (Fig. 1). Upper aerodigestive tract infections begin within the pharyngeal mucosal space and may spread to the deep spaces of the neck if not appropriately treated. Infections that involve the pharyngeal mucosal space include pharyngitis, tonsillitis, peritonsillar abscess, and epiglottis.

In patients with acute tonsillitis, the affected tonsillar tissue is enlarged and enhances after contrast material administration. The tonsils may display a striated enhancement pattern (tiger-stripe appearance), reflecting inflamed enhancing mucosa with underlying edematous submucosa. Uvulitis, enlargement and inflammation involving the uvula may be an associated finding (Fig. 2A). Uncomplicated tonsillitis will not have a localized region of internal hypoattenuation. As the infection progresses, an ill-defined region of hypoattenuation without a well-defined enhancing wall representing cellulitis or phlegmon may develop within the tonsil. This process may continue to evolve to abscess formation, defined by a low-density collection with attenuation similar to CSF surrounded by an enhancing wall. These abscesses may uncommonly remain within the tonsillar tissue, a true intratonsillar abscess. The majority of these abscesses will penetrate the fibrous capsule of the tonsil to involve the potential space located between the superior constrictor muscle and tonsillar capsule, termed a peritonsillar abscess [2] (Fig. 2B).

Because treatment of peritonsillar abscess differs from acute tonsillitis and cellulitis or phlegmon, accurate characterization is paramount. The detection of a peritonsillar abscess requires incision and drainage or aspiration of the drainable fluid collection in addition to antibiotic therapy. Clinical assessment has low specificity for differentiating tonsillar cellulitis from peritonsillar abscess. Even when strict imaging criteria are applied, accurate detection of drainable fluid collections on contrast-enhanced CT ranges from 63% to 77% in both adult and pediatric populations [7, 8]. An irregular or scalloped morphology of the enhancing wall of a fluid collection increases the specificity for abscess and suggests a more mature abscess [9] (Fig. 2C).

Epiglottitis and supraglottitis are inflammation of the epiglottis and adjacent supraglottic larynx, respectively, that is typically caused by bacteria. Historically, this condition was more frequent in children infected with *Haemophilus influenzae* type b (HIB). However, since widespread childhood vaccination to HIB was introduced in the 1990s, acute epiglottitis is now more frequent

[1]Both authors: Department of Medical Imaging, University of Arizona, 1501 Campbell Ave, PO Box 245067, Tucson, AZ 85724. Address correspondence to W. S. Kubal (wkubal@email.arizona.edu).

in adults and is caused by a variety of bacterial pathogens, including *Streptococcus* species and *Staphylococcus aureus* [10]. Symptoms include sore throat, fever, muffled voice, drooling, stridor or respiratory compromise, and hoarseness. Definitive diagnosis is made by direct visualization, which may require laryngoscopy. Treatment includes maintaining a patent airway, corticosteroids, and IV antibiotics.

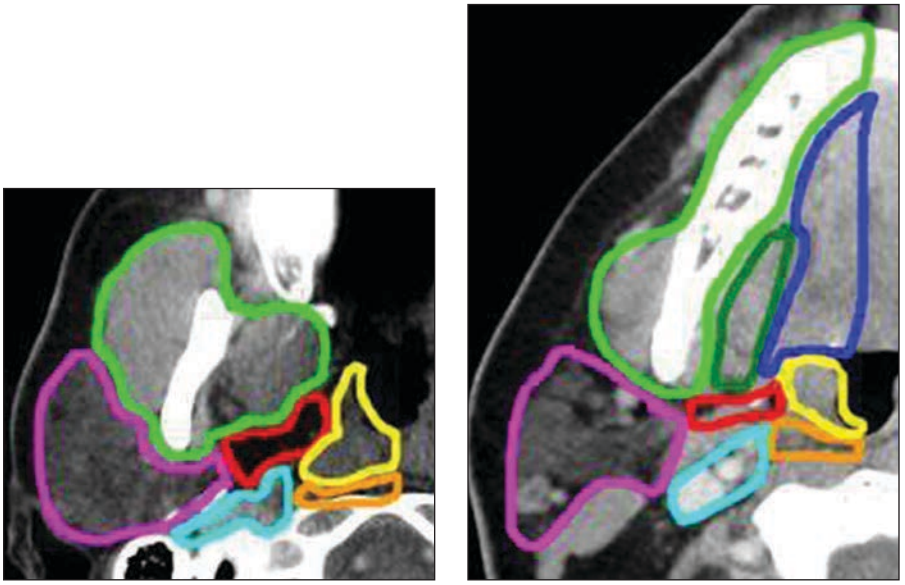

Fig. 1—Spaces of neck. (Reprinted from *Radiol Clin North Am* Vol. 53, Kubal WS, Face and neck infections: what the emergency radiologist needs to know, 827–846, Copyright 2015, with permission from Elsevier)
A, Axial contrast-enhanced CT image shows pharyngeal mucosal space (*yellow*), retropharyngeal space (*orange*), masticator space (*light green*), parotid space (*magenta*), parapharyngeal space (*red*), and carotid space (*light blue*).
B, Axial contrast-enhanced CT image caudal to **A** shows two additional spaces: sublingual space (*dark blue*) and submandibular space (*dark green*).

Historically, lateral radiographs have been used as a first-line imaging modality for the detection of epiglottitis. Findings include thickening of the epiglottis ("thumb" sign), obliteration of the valleculae ("vallecula" sign), thickening of the aryepiglottic folds, and dilatation of the hypopharynx. Contrast-enhanced CT is useful in diagnosis of epiglottis when direct visualization is not feasible. CT can differentiate epiglottitis from other causes of fever and sore throat (e.g., tonsillar abscess, retropharyngeal abscess) and allows characterization of complicating features (e.g., abscess formation, soft-tissue gas, airway compromise). The CT findings of epiglottitis include swelling of the epiglottis and supraglottic structures (e.g., aryepiglottic folds, false vocal cords), inflammatory stranding of the preepiglottic fat, and thickening of the platysma and prevertebral fascia (Fig. 3) [11].

The Retropharyngeal Space

The retropharyngeal space is a small space containing predominantly fat situated between the posterior aspect of the pharyngeal mucosal space and cervical esophagus and anterior to the prevertebral musculature (Fig. 1). The suprahyoid retropharyngeal space contains medial

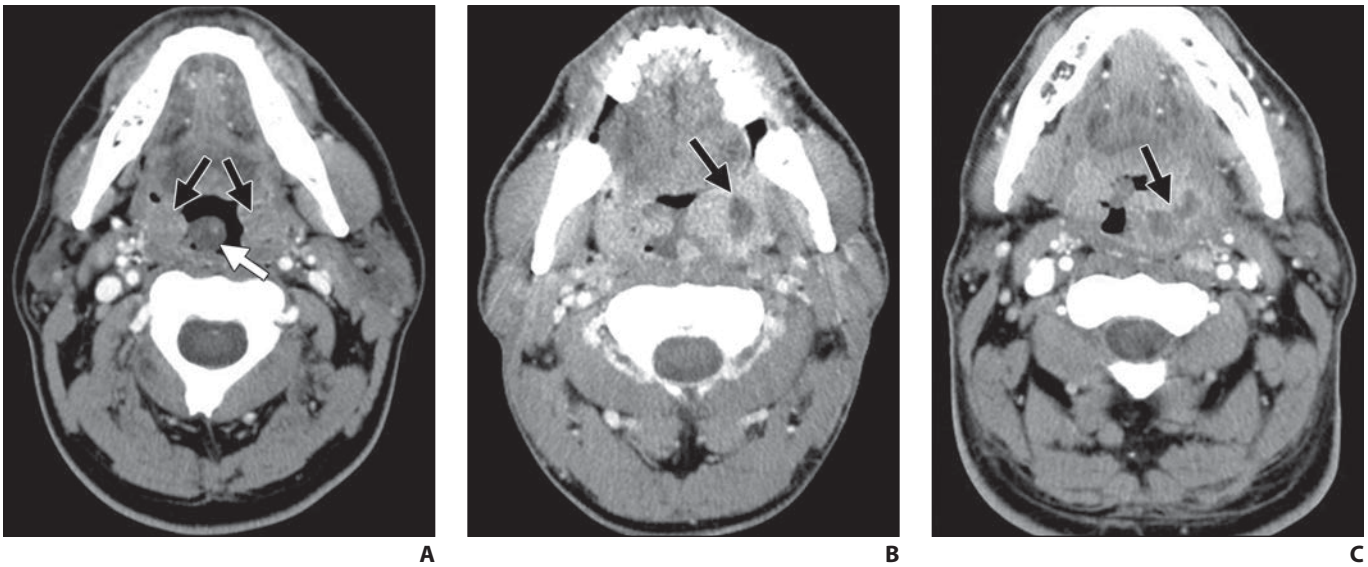

Fig. 2—Axial contrast-enhanced CT images in three different patients show infections within pharyngeal mucosal space. (Reprinted from *Radiol Clin North Am* Vol. 53, Kubal WS, Face and neck infections: what the emergency radiologist needs to know, 827–846, Copyright 2015, with permission from Elsevier)
A, Tonsils are enlarged and show increased enhancement bilaterally (*black arrows*). Enhancement pattern is striated (resembling tiger stripes). Uvula appears enlarged and edematous (*white arrow*). These findings are compatible with acute tonsillitis.
B, Area of decreased density with enhancing rim involving left tonsil (*arrow*) is seen in this patient. This finding is compatible with peritonsillar abscess.
C, Area of decreased density is seen with enhancing, scalloped rim involving left tonsil (*arrow*) is seen in this patient. This finding is compatible with abscess seen in **B**.

and lateral retropharyngeal lymph nodes, which are more prominent in children less than 6 years old [12]. The retropharyngeal space has a bowtie configuration with variable presence of a median raphe, more often superiorly, which may confine disease to half of the space. The retropharyngeal space extends from the clivus to terminate between the T1 and T6 vertebral levels. The danger space is a potential space located posterior to the retropharyngeal space separated from it by the thin posterior slip of the alar fascia, which extends inferiorly to the diaphragm. Infection within the retropharyngeal space or within the danger space may extend from the pharynx to the mediastinum [13]. It is therefore crucial to detect an infection within the retropharyngeal space and evaluate the superior mediastinum for the potential complication of mediastinitis (Fig. 4). Infections within the retropharyngeal space may result from lymphatic spread of pharyngeal infections, cervical discogenic infections, or penetrating trauma.

On contrast-enhanced CT, retropharyngeal abscess is defined by low-attenuation fluid filling the retropharyngeal space with a surrounding enhancing wall. The abscess typically shows mass effect on the walls from the increased internal pressure. These findings contrast those of suppurative retropharyngeal lymphadenitis, typically encountered in the pediatric population, which are focal, rim-enhancing fluid collections along the lateral margins of the suprahyoid retropharyngeal space. Retropharyngeal abscesses require surgical drainage. Patients with suppurative retropharyngeal lymphadenitis typically receive a trial of IV antibiotics for 24–48 hours when the collection measures less than 2 cm^3 in size. Surgical drainage is reserved for recalcitrant cases [14].

Calcific tendinitis of the longus colli muscle is an inflammatory condition that may mimic the clinical presentation (e.g., neck pain and fever) and some imaging findings of retropharyngeal abscess. On contrast-enhanced CT, this entity typically shows fluid or edema within the retropharyngeal space. In contrast to retropharyngeal abscess, the walls of the retropharyngeal space do not enhance in the setting of calcific tendinitis [15, 16]. In addition, amorphous calcification is present in the tendinous insertion of the longus colli muscle, typically seen along the inferior margin of the anterior arch of C1. Calcium hydroxyapatite crystal deposition is responsible for inciting the inflammation (Fig. 5). Differentiation of calcific tendinitis of the longus colli muscle from retropharyngeal abscess is essential, because treatment of the tendonitis is nonsurgical with nonsteroidal antiinflammatory medications.

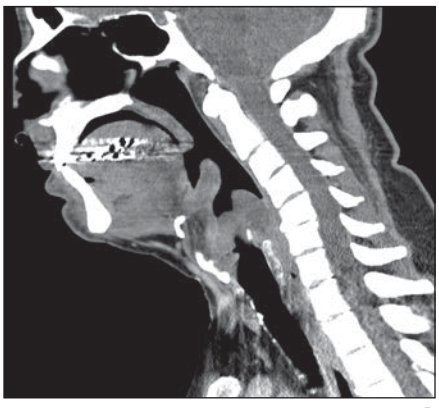

A

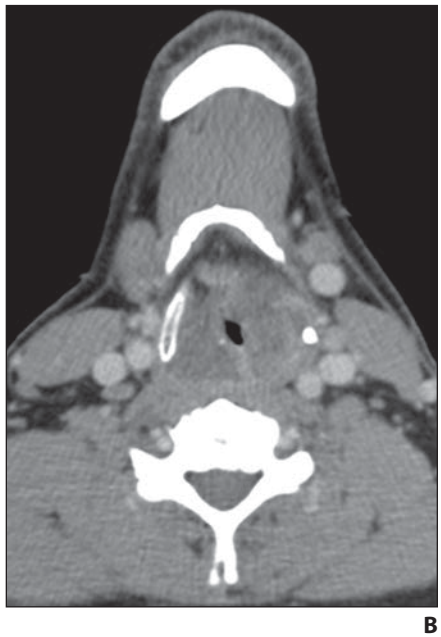

B

Fig. 3—Epiglottitis. (Reprinted from *Radiol Clin North Am* Vol. 53, Kubal WS, Face and neck infections: what the emergency radiologist needs to know, 827–846, Copyright 2015, with permission from Elsevier)
A, Contrast-enhanced sagittal CT image shows thickened epiglottis and supraglottis with preepiglottic fat stranding.
B, Contrast-enhanced axial CT image shows submucosal edema within false vocal cords and aryepiglottic folds.

The Masticator Space

The masticator space includes the muscles of mastication and portions of the adjacent posterior mandible (Fig. 1). Because the masticator space contains the posterior mandible, infections are typically odontogenic in origin, spreading from dental abscesses or following dental procedures involving the posterior mandibular molars. Because the deep cervical fascia surrounds all the muscles of mastication, infections can spread superiorly along the temporalis muscle above the zygomatic arch into the suprazygomatic masticator space to its attachment to the parietal calvaria. This fact may necessitate more superior imaging coverage to examine the entirety of the masticator space.

On contrast-enhanced CT, infections within the masticator space may show swelling of the affected muscles, variable enhancement, adjacent fat stranding, and possible rim-enhancing fluid collections. Careful evaluation of the adjacent posterior mandibular teeth on bone algorithm images can often identify the infectious source as evidenced by periapical lucency with or without cortical breach or the site of a recent dental procedure. Irregularity of the bone may reflect osteomyelitis, a complication of masticator space infection that requires aggressive antibiotic therapy.

Subtle deep masticator space infections involving the pterygoid muscles may be associated with inflammatory disease in the adjacent maxillary sinuses. Identification of infection in this location should be considered when inflammatory stranding is seen in the fat of the pterygopalatine fossa or retroantral fat pad situated between the maxillary sinus and masticator space (Fig. 6).

The Parotid Space

The parotid gland and its intraparotid lymph nodes are surrounded by the superficial layer of the deep cervical fascia forming the parotid space (Fig. 1). The parotid

gland can vary in internal attenuation but normally has lower density than muscle and higher density than the subcutaneous fat on contrast-enhanced CT.

Parotid gland infections may result from bacterial or viral agents. Bacterial infections are often unilateral and assumed to result from an ascending infection from the oral cavity. These infections are easy to identify both clinically and on contrast-enhanced CT because there is a normal parotid gland for comparison. Imaging shows unilateral enlargement and contrast enhancement of the affected parotid gland with surrounding inflammatory fat stranding. CT is particularly useful in the detection of a focal rim-enhancing fluid collection, compatible with intraparotid abscess, or a potential hyperattenuating calculus obstructing the parotid (Stensen) duct.

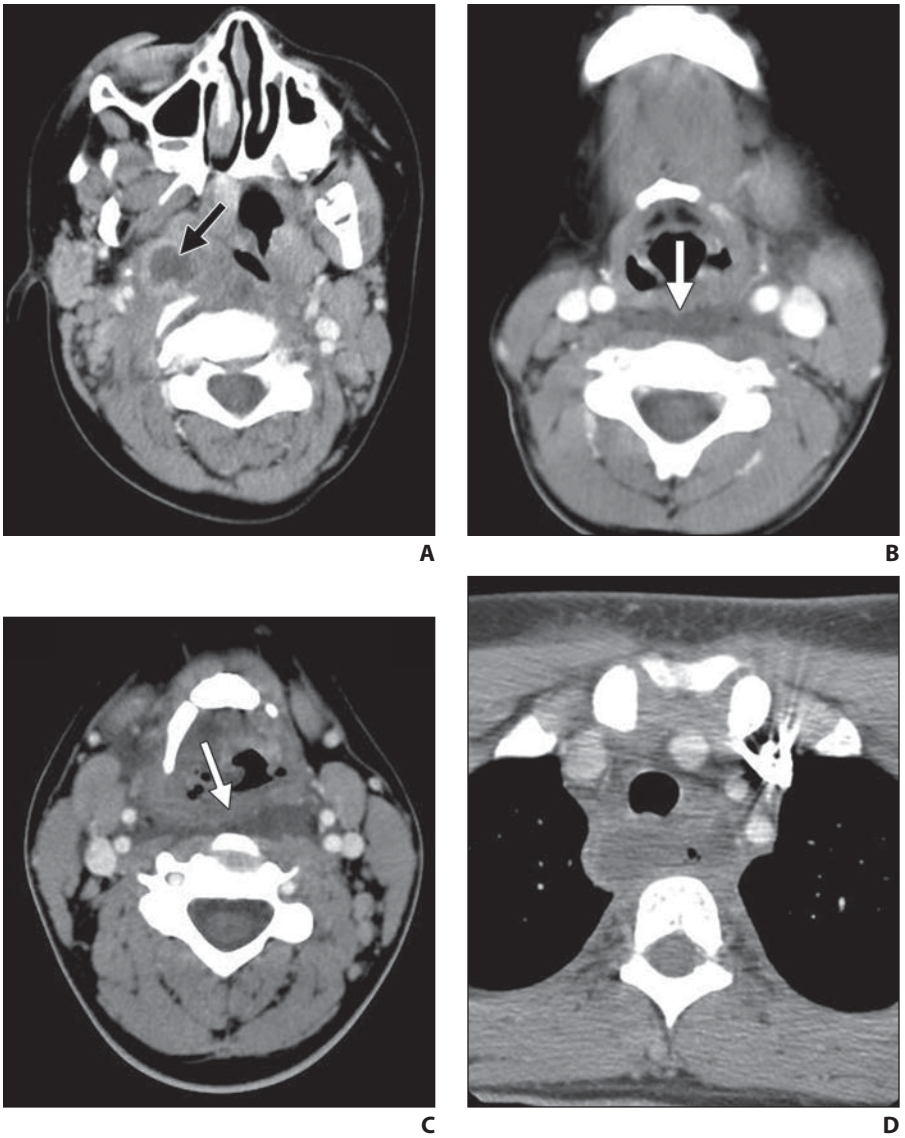

Fig. 4—Infection within pharyngeal mucosal space spreading to retropharyngeal space and extending to mediastinum.
A, Axial contrast-enhanced CT shows well-defined low density collection within right tonsillar region consistent with peritonsillar abscess (*arrow*).
B, Axial contrast-enhanced CT at lower level in neck shows persistent, low-density edema within retropharyngeal space. This image shows bowtie configuration characteristic of retropharyngeal space (*arrow*).
C, Axial contrast-enhanced CT at level of hyoid bone shows persistent edema within retropharyngeal space (*arrow*).
D, Axial contrast-enhanced CT at level of mediastinum shows infection extending into superior mediastinum. Findings on this section are compatible with mediastinitis.

Viral parotitis is typically bilateral (e.g., mumps) and occurs in approximately 75% of cases [2]. These cases may be difficult to diagnose given the lack of a normal parotid gland for comparison. Increased attenuation of the parotid glands when compared with muscle and adjacent fat stranding will aid in the diagnosis.

The Carotid Space

Portions of the deep cervical fascia loosely invest the internal jugular vein, carotid artery, portions of cranial nerves IX–XII, and adjacent internal jugular chain lymph nodes (Fig. 1). It is important to evaluate both the internal jugular vein and carotid arteries when assessing the carotid space. These vessels are readily identified on a contrast-enhanced examination. The internal jugular vein typically is located along the posterolateral margins of the carotid arteries. Detection of inflammatory fat stranding along the margins of these vessels may indicate carotid space infection.

In 1936, Andre Lemierre [17] reported a case series in which septicemia resulted from anaerobic organisms found physiologically in the human body. Lemierre syndrome (LS) describes septic thrombophlebitis of the internal jugular vein, typically the result of oropharyngeal infection. This infection may also result in septic emboli, most commonly to the lungs [18]. On contrast-enhanced CT, expansion and lack of contrast opacification of the internal jugular vein with surrounding inflammatory fat stranding is indicative of septic thrombophlebitis (Fig. 7A). CT may also show the causative oropharyngeal infection (e.g., peritonsillar abscess). When septic thrombophlebitis is detected, the lungs should be evaluated for cavitary nodules indicative of septic emboli (Fig. 7B). According to Weeks et al. [18], "given the relatively low incidence of LS and its potentially confusing clinical manifestations, recognition of imaging findings consistent with the diagnosis may be crucial to rendering a timely diagnosis and institution of appropriate therapy, and the radiologist may be the initial physician to suggest or establish the diagnosis."

Infectious arteritis affecting the cervical portions of the carotid arteries is rare but may result in significant morbidity and mortality. This infection may be a direct

extension from external infection (e.g., retropharyngeal abscess) or of hematogenous origin (e.g., septic emboli). Weakening of the carotid wall by proteolytic enzymes or thrombosis of the vasa vasorum can lead to pseudoaneurysm formation (Fig. 8) or carotid rupture. Suspected infectious arteritis of the carotid artery, particularly with associated pseudoaneurysm, should be emergently communicated to the treating physician given the dire consequences of a potential carotid rupture. Patients may be treated with stent placement, endovascular occlusion, or surgical bypass [19].

The Sublingual Space

The paired sublingual spaces are the lateral aspects of the floor of mouth that lie inferior to the intrinsic tongue muscles, superomedial to the mylohyoid muscle, and lateral to the geniohyoid-genioglossus complex (Fig. 1B). These spaces contain the sublingual glands, small portions of the superior submandibular glands, the submandibular ducts, tongue neurovascular bundles, hyoglossus muscles, and fat. The roots of the second and third molars

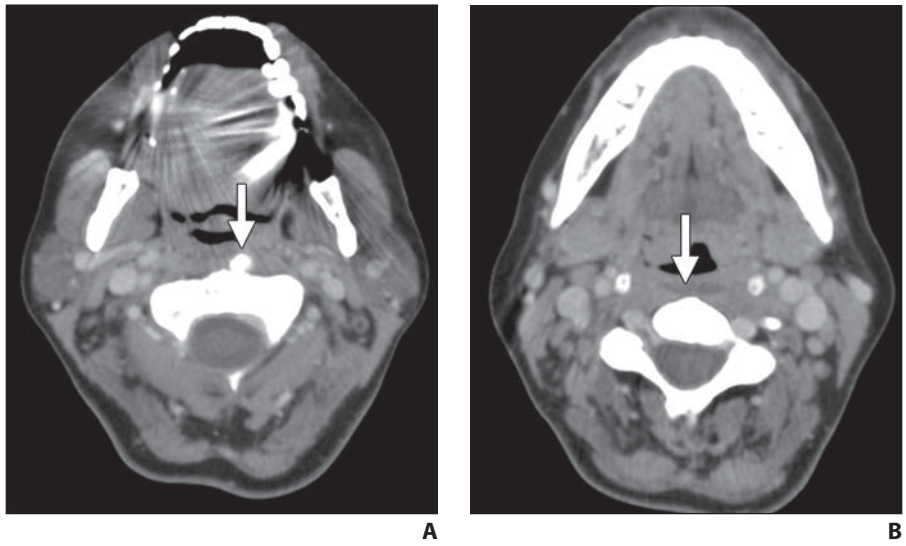

Fig. 5—Calcific tendinitis of longus colli with edema within retropharyngeal space. (Reprinted from *Radiol Clin North Am* Vol. 53, Kubal WS, Face and neck infections: what the emergency radiologist needs to know, 827–846, Copyright 2015, with permission from Elsevier)
A, Axial contrast-enhanced CT shows calcification anterior to C2 vertebral body (*arrow*). This calcification lies at superior insertion of longus colli muscle.
B, Axial contrast-enhanced CT caudal to **A** shows small amount of fluid and edema is present within retropharyngeal space (*arrow*). Fluid is secondary to calcific tendinitis rather than due to infection.

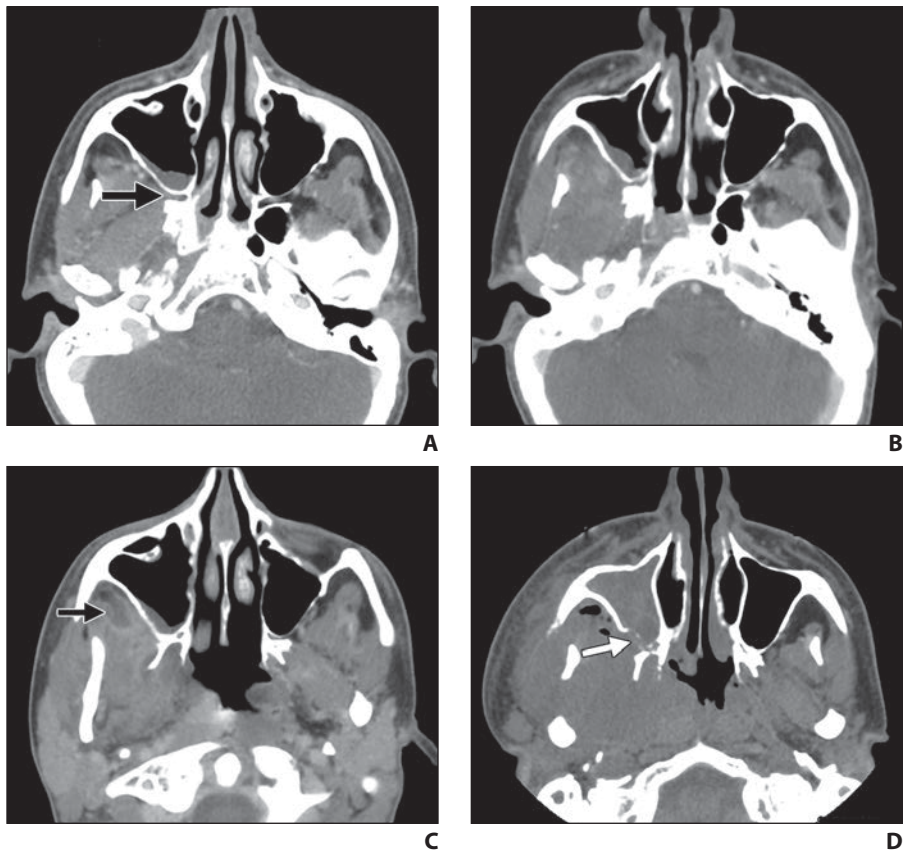

Fig. 6—Series of contrast-enhanced axial CT scans show progression of right masticator space infection. (Reprinted from *Radiol Clin North Am* Vol. 53, Kubal WS, Face and neck infections: what the emergency radiologist needs to know, 827–846, Copyright 2015, with permission from Elsevier)
A, Patient initially presented with right facial pain. Small amount of sinus disease is noted within right maxillary sinus. Important, but more subtle, finding that was not initially appreciated is infiltration of fat within right pterygopalatine fossa (*arrow*).
B, Approximately 3 weeks later, patient returns with increased right facial pain. Swelling and patchy areas of abnormal enhancement within right masticator space are now easily appreciated.
C, Despite IV antibiotic therapy, patient continues to worsen. CT image shows early suppuration (*arrow*) just anterior to mandible.
D, Subsequent CT image shows infection has spread to adjacent spaces with involvement of superficial face, opacification of right maxillary sinus, and extension to right pharyngeal mucosal space. There is also bone destruction involving posterior wall of maxillary sinus (*arrow*) consistent with osteomyelitis.

extend below the insertion of the mylohyoid muscle, so infections of those teeth are likely to involve the submandibular space [2]. Because the roots of the teeth anterior to the second molar extend above the mylohyoid muscle, infections of those teeth typically are contained in the sublingual space [2].

Ludwig angina, a potentially life-threatening cellulitis involving the floor of mouth and adjacent submandibular spaces, is typically the consequence of odontogenic infection. The infection extends to involve multiple spaces and may result in airway compromise. On contrast-enhanced CT, inflammatory stranding and edema affect the sublingual and submandibular spaces, which are particularly well visualized on coronal reformatted images. Soft-tissue gas and rim-enhancing fluid collections may also be present.

The Submandibular Space

The submandibular space lies inferolateral to the mylohyoid muscle and deep to the platysma (Fig. 1B) and contains predominantly the submandibular glands, lymph nodes, and fat. Posterior to the mylohyoid muscle attachment, the submandibular space communicates with the sublingual and parapharyngeal spaces. Odontogenic infections involving the second or third mandibular molars may extend into the submandibular spaces because these dental roots reside below the attachment of the mylohyoid sling. Submandibular space abscesses are rim-enhancing, low-density fluid collections with surrounding inflammatory fat stranding that often connect to a posterior mandibular periapical lucency via an osseous dehiscence.

In addition, infections may be centered within the submandibular glands, resulting in sialadenitis. These bacterial infections will appear similar to their counterparts in the parotid glands, with asymmetric enlargement, enhancement, and surrounding inflammatory fat stranding of the affected submandibular gland. A hyperdense calculus may also be seen on CT along the expected course of the submandibular (Wharton) duct and proximal ductal dilatation in the setting of obstructive sialolithiasis.

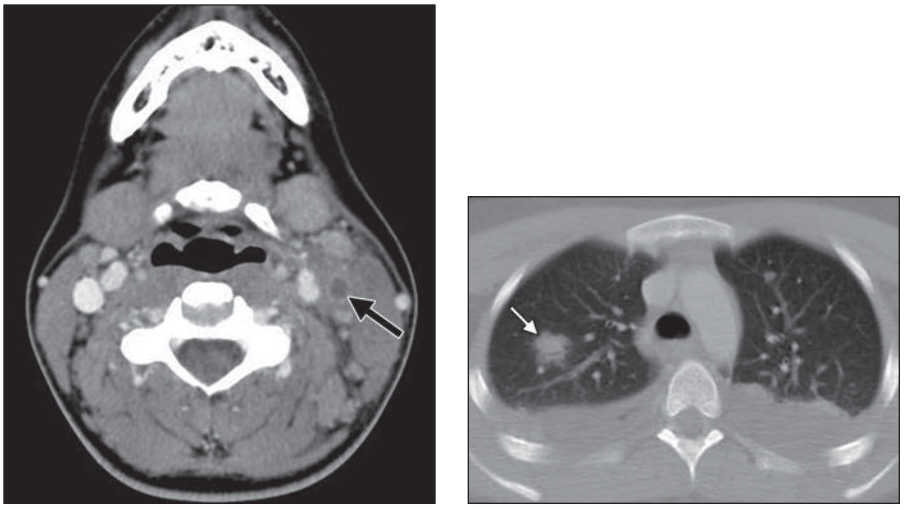

A B

Fig. 7—Lemierre syndrome. (Reprinted from *Radiol Clin North Am* Vol. 53, Kubal WS, Face and neck infections: what the emergency radiologist needs to know, 827–846, Copyright 2015, with permission from Elsevier)
A, Right carotid artery and internal jugular vein appear normal on contrast-enhanced axial CT image of neck. On left there is nonfilling of lumen of internal jugular vein, abnormal enhancement of wall of jugular vein, and fat infiltration surrounding jugular vein (*arrow*). These findings are compatible with septic thrombophlebitis involving left internal jugular vein.
B, Contrast-enhanced axial CT image of chest shows bilateral pleural effusions as well as right lung opacity (*arrow*). Right lung opacity represents septic embolus.

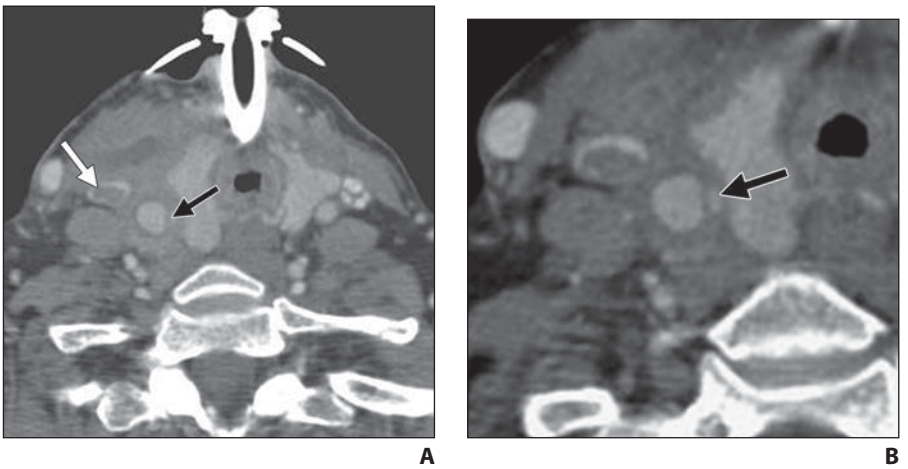

A B

Fig. 8—Infection and common carotid artery pseudoaneurysm. (Reprinted from *Radiol Clin North Am* Vol. 53, Kubal WS, Face and neck infections: what the emergency radiologist needs to know, 827–846, Copyright 2015, with permission from Elsevier)
A, Contrast-enhanced axial CT image of neck shows postoperative changes, fluid collection within right neck, and infiltration of fat within right carotid space. Thrombus is present within right internal jugular vein (*white arrow*). Right common carotid artery appears abnormal with small collection of contrast seen at its medial margin (*black arrow*).
B, 1.5x magnified view of right common carotid shows contrast filling structure medial to vessel (*arrow*). This finding is compatible with carotid pseudoaneurysm.

Congenital Lesions

Second branchial cleft cysts are congenital fluid-filled lesions within the submandibular spaces characteristically located posterior to the submandibular gland, deep to the sternocleidomastoid muscle, and anterolateral to the carotid artery. These lesions may become clinically apparent when secondarily infected. CT shows a rim-enhancing fluid collection with surrounding stranding in the characteristic location. Metastatic cervical lymphadenopathy in the setting of head and neck squamous cell carcinoma related to hu-

man papillomavirus infection may have an identical imaging appearance and should be the top differential diagnostic consideration in patients outside of the pediatric or adolescent age groups.

Lymphatic malformations are congenital slow-flow vascular malformations composed of abnormal lymphatic channels. These lesions may become clinically evident when they are secondarily infected. On contrast-enhanced CT, lymphatic malformations are transspatial, multiseptated cystic lesions without wall enhancement. When infected, these malformations show wall and septal thickening and enhancement and can resemble a complex abscess.

Summary

The detection, characterization, localization, classification of potential complications, and recognition of causes of head and neck infections are each critical roles of the emergency radiologist. Knowledge of normal head and neck anatomy and CT appearance will not only aid in detection of subtle infection and space of origin but also help in predicting potential patterns of spread, complications, and cause. Because soft-tissue infections lie on a spectrum from cellulitis to drainable abscess, knowledge of the contrast-enhanced CT appearances of these different stages allows appropriate medical or surgical management for the underlying head and neck infection. The information provided should help the radiologist "to provide an accurate and prompt diagnosis, assess the extent of disease, evaluate for potential complications, and recommend definitive subspecialty evaluation" [2].

REFERENCES

1. Maroldi R, Farina D, Ravanelli M, et al. Emergency imaging assessment of deep neck space infections. *Semin Ultrasound CT MR* 2012; 33:432–442
2. Capps EF, Kinsella JJ, Gupta M, et al. Emergency imaging assessment of acute, nontraumatic conditions of the head and neck. *RadioGraphics* 2010; 30:1335–1352
3. Wang B, Gao BL, Xu GP, Xiang C. Images of deep neck space infection and the clinical significance. *Acta Radiol* 2014; 55:945–951
4. Crespo AN, Chone CT, Fonseca AS, et al. Clinical versus computed tomography evaluation in the diagnosis and management of deep neck infection. *Sao Paulo Med J* 2004; 122:259–263
5. Scott BA, Stiernberg CM, Driscoll BP. Deep neck space infections. In: Bailey BJ, ed. *Head and neck surgery: otolaryngology*, 2nd ed. Philadelphia, PA: Lippincott-Raven, 1998:819–835
6. Kubal WS. Face and neck infections: what the emergency radiologist needs to know. *Radiol Clin North Am* 2015; 53:827–846
7. Vural C, Gungor A, Comerci S. Accuracy of computerized tomography in deep neck infections in the pediatric population. *Am J Otolaryngol* 2003; 24:143–148
8. Miller WD, Furst IM, Sàndor GKB, Keller MA. A prospective, blinded comparison of clinical examination and computed tomography in deep neck infections. *Laryngoscope* 1999; 109:1873–1879
9. Kirse DJ, Roberson DW. Surgical management of retropharyngeal space infections in children. *Laryngoscope* 2001; 111:1413–1422
10. Mayo-Smith MF, Spinale JW, Schiffman FJ, et al. Acute epiglottitis: an 18-year experience in Rhode Island. *Chest* 1995; 108:1640–1647
11. Smith MM, Mukherji SK, Thompson JE, et al. CT in adult supraglottitis. *AJNR* 1996; 17:1355–1358
12. Virk JS, Pang J, Okhovat S, Lingam RK, Singh A. Analyzing lateral soft tissue neck radiographs. *Emerg Radiol* 2012; 19:255–260
13. Debnam JM, Guha-Thakurta N. Retropharyngeal and prevertebral spaces: anatomic imaging and diagnosis. *Otolaryngol Clin North Am* 2012; 45:1293–1310
14. Shefelbine SE, Mancuso AA, Gajewski BJ, et al. Pediatric retropharyngeal lymphadenitis: differentiation from retropharyngeal abscess and treatment implications. *Otolaryngol Head Neck Surg* 2007; 136:182–188
15. Eastwood JD, Hudgins PA, Malone D. Retropharyngeal effusion in acute calcific prevertebral tendinitis: diagnosis with CT and MR imaging. *AJNR* 1998; 19:1789–1792
16. Chung T, Rebello R, Gooden EA. Retropharyngeal calcific tendinitis: case report and review of literature. *Emerg Radiol* 2005; 11:375–380
17. Lemierre A. On certain septicæmias due to anaerobic organisms. *Lancet* 1936; 227:701–703
18. Weeks DF, Katz DS, Saxon P, Kubal WS. Lemierre syndrome: report of five new cases and literature review. *Emerg Radiol* 2010; 17:323–328
19. Hirai T, Korogi Y, Sakamoto Y, et al. Emergency balloon embolization for carotid artery rupture secondary to postoperative infection. *Cardiovasc Intervent Radiol* 1996; 19:50–52